DALTON
FULL PAPER

Aspects of the co-ordination chemistry of the antiviral nucleotide analogue, 9-[2-(phosphonomethoxy)ethyl]-2,6-diaminopurine (PMEDAP)

Claudia A. Blindauer,[a] Trond I. Sjåstad,[b] Antonín Holý,[c] Einar Sletten[b] and Helmut Sigel*[a]

[a] *Institute of Inorganic Chemistry, University of Basel, Spitalstrasse 51, CH-4056 Basel, Switzerland. E-mail: Sigel@ubaclu.unibas.ch*
[b] *Department of Chemistry, University of Bergen, N-5007 Bergen, Norway*
[c] *Institute of Organic Chemistry and Biochemistry, Academy of Sciences, CZ-16610 Prague, Czech Republic*

Received 17th June 1999, Accepted 23rd July 1999

The acidity constants of the twofold protonated, acyclic, antiviral nucleotide analogue 9-[2-(phosphonomethoxy)-ethyl]-2,6-diaminopurine, $H_2(PMEDAP)^{\pm}$, as well as the stability constants of the M(H;PMEDAP)$^+$ and M(PMEDAP) complexes with the metal ions M^{2+} = Mg^{2+}, Ca^{2+}, Sr^{2+}, Ba^{2+}, Mn^{2+}, Co^{2+}, Ni^{2+}, Cu^{2+}, Zn^{2+} or Cd^{2+}, have been determined by potentiometric pH titrations in aqueous solution at I = 0.1 M ($NaNO_3$) and 25 °C. Application of previously determined straight-line plots of log $K^{M}_{M(R\text{-}PO_3)}$ *versus* p$K^{H}_{H(R\text{-}PO_3)}$ for simple phosph(on)ate ligands and comparisons with previous results obtained for the nucleobase-free compound (phosphonomethoxy)-ethane, PME, and its derivative, PME-R, where R represents a nucleobase residue without an affinity for metal ions, show that the primary binding site of $PMEDAP^{2-}$ is the phosphonate group with all the metal ions studied and that also in all instances 5-membered chelates involving the ether oxygen of the $-CH_2OCH_2PO_3^{2-}$ chain are formed. The position of the isomeric equilibria between these chelates, $M(PMEDAP)_{cl/O}$, and the 'open' complexes, $M(PMEDAP)_{op}$, is determined. In the M^{2+}/$PMEDAP^{2-}$ systems with Co^{2+}, Ni^{2+}, Cu^{2+}, and most likely also Zn^{2+}, a third isomer is formed which was detected by comparing the stabilities of the M(PMEDAP) and M(PME-R) complexes; this additional stability enhancement has to be attributed to the 2,6-diaminopurine residue. General considerations as well as ^{1}H NMR line broadening studies with Cu^{2+} reveal that in this third isomer a macrochelate is formed in which the phosphonate-bound metal ion interacts in addition with N7 of the purine residue, $M(PMEDAP)_{cl/N7}$. The equilibria involving the three isomers are described and quantified; *e.g.* 19 (±3)% of Cu(PMEDAP) exists as an isomer with a sole phosphonate co-ordination, 38 (±11)% as $Cu(PMEDAP)_{cl/O}$ and 43 (±11)% as $Cu(PMEDAP)_{cl/N7}$. The corresponding numbers of Ni(PMEDAP) are 33 (±6)% (open), 13 (±8)% (cl/O) and 54 (±10)% (cl/N7). The open and the macrochelated isomers resemble in their structure the corresponding complexes formed by the parent nucleotide adenosine 5′-monophosphate (AMP^{2-}). The possible interrelation between the structure of the metal ion complexes in solution and the antiviral properties of PMEDAP and related compounds is discussed.

Introduction

So-called acyclic nucleoside phosphonates (ANPs)[1,2] represent a structural class of (2′-deoxy)nucleoside 5′-monophosphate analogues,[2–4] in which the ribose phosphate residue is replaced by an aliphatic chain with a phosphonate group. These nucleotide analogues are among the most promising novel compounds with antiviral properties.[2–5] They exhibit activity against a variety of DNA viruses,[6] some of them also against retroviruses, including human immunodeficiency viruses (HIV).[7] The prototype of this class of substances, 9-[2-(phosphonomethoxy)ethyl]adenine (PMEA; Fig. 1), is currently under clinical investigation in the form of a prodrug, *i.e.* an easily hydrolysable diester which facilitates cellular uptake.[8]

The metabolism of several ANPs has been studied and it is now known that their biological activity is based on their diphosphorylated derivatives,[9–12] ANPpp, which can be considered as analogues of (2′-deoxy)nucleoside 5′-triphosphates. They are generated by cellular enzymes[11] and act as alternative substrates for DNA polymerases.[9,13] These species, which can also be considered as derivatives of phosphonomethoxyethane (PME; Fig. 1), are inserted in the growing DNA chain and since they lack the equivalent of the 3′-OH group present in the corresponding nucleotides (for examples see Fig. 1) the further growth of the DNA chain is terminated.[14] The ANPpp species

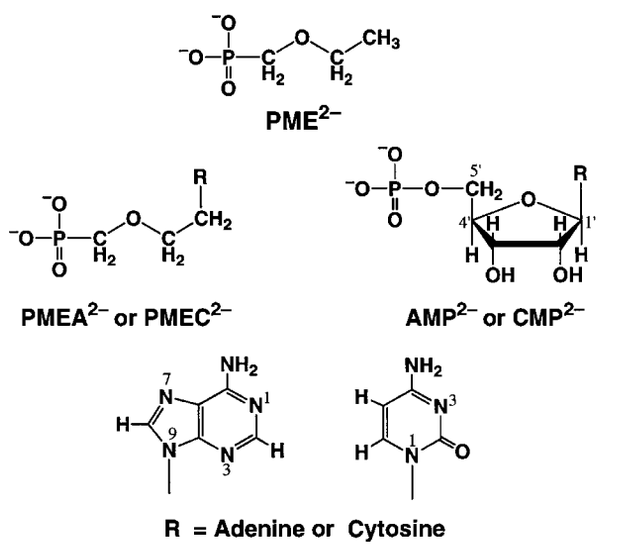

Fig. 1 Chemical structure of the dianion of phosphonomethoxy-ethane (PME^{2-}), as well as of its derivatives 9-[2-(phosphonomethoxy)-ethyl]adenine ($PMEA^{2-}$) and 1-[2-(phosphonomethoxy)ethyl]cytosine ($PMEC^{2-}$). The structures of the parent nucleotides adenosine 5′-monophosphate (AMP^{2-}) and cytidine 5′-monophosphate (CMP^{2-}) are shown for comparison.

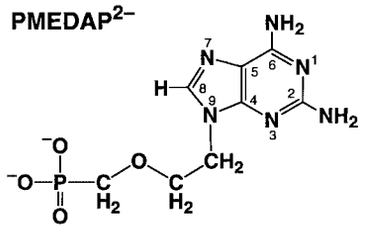

Fig. 2 Chemical structure of the dianion of 9-[2-(phosphonomethoxy)ethyl]-2,6-diaminopurine ($PMEDAP^{2-}$).

usually affect viral DNA polymerases considerably more than the cellular enzymes of the host.[15]

It is our aim to contribute to the elucidation of the structure–activity relationship of ANPs by determining some of their principal properties, such as their acid–base behavior,[16] as well as their affinity toward metal ions and the structures of the resulting metal ion complexes in solution,[17–20] and to further our understanding by comparing their properties with those of their natural parent compounds, *i.e.* the (2′-deoxy)nucleoside 5′-monophosphates [(d)NMPs; *cf.*, *e.g.*, Fig. 1].[21,22] Studies concerning metal ion complexes are of relevance, since it is well known that metal ions, especially Mg^{2+}, are generally involved in the metabolism of nucleotides[23,24] and DNA polymerases,[25] the latter being ultimate targets of the ANPs.

One of the main results of our studies is that we could prove that the metal ion complexes formed with[17–20] $PMEA^{2-}$ and the cytosine derivative $PMEC^{2-}$ (Fig. 1)[26] differ in part in their structure in solution from that of the complexes of their parent nucleotides[21,22] AMP^{2-} and CMP^{2-} (Fig. 1) in so far that the involvement of the ether oxygen atom in metal ion binding gives rise to the formation of 5-membered chelates and thus to the intramolecular equilibrium (1).[17–20] This feature, together

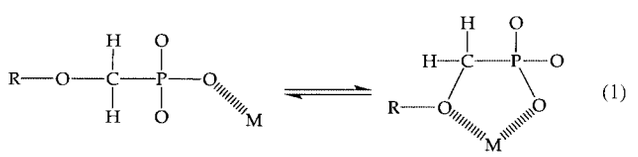

with the increased basicity of a phosphonyl group (compared to that of a phosphoryl group),[27] leads to an increased complex stability as we could prove by studying the complexes of methylphosphonylphosphate, $CH_3P(O)_2^-$–O–PO_3^{2-}.[28] Both facts together led us to conclude[29] that metal ion binding to the α-phosph(on)ate group in $ANPpp^{4-}$ is favored over that in NTP^{4-} and that this makes the $M_2(ANPpp)$ complexes the preferred initial substrates for the target DNA polymerases.

During biochemical studies regarding the structure–activity relationship, the 2-amino derivative of PMEA, *i.e.* 9-[2-(phosphonomethoxy)ethyl]-2,6-diaminopurine (PMEDAP; Fig. 2), emerged as a potentially useful antiviral compound.[3,4,30] Indeed, recently the methyl derivative of PMEDAP, *i.e.*, (*R*)-9-[2-(phosphonomethoxy)propyl]-2,6-diaminopurine (PMPDAP), was shown to be an even more potent inhibitor of HIV replication than PMEA, having a remarkably low cytotoxicity.[31] PMEDAP itself shows a similar activity spectrum but is slightly more active than PMEA against several DNA viruses (herpes virus, hepadna virus) and retroviruses (HIV-1 and 2, Moloney murine sarcoma virus).[31] In addition, PMEDAP has, compared to PMEA, a more pronounced cytostatic effect; it affects the growth of mouse and human leukemia cell lines.[32] It has also been shown that PMEDAPpp selectively inhibits[14a] the cellular DNA polymerase δ, which is involved in eukaryotic genome replication. These interesting biological features of PMEDAP prompted us to include this compound in our studies and we are reporting now the acid–base properties of $H(PMEDAP)^-$ as well as its metal ion-binding properties toward the alkaline earth ions, several 3d metal ions, Zn^{2+} and Cd^{2+}.

Experimental

Materials

The free acid of 9-[2-(phosphonomethoxy)ethyl]-2,6-diaminopurine was synthesized according to published procedures.[33] The aqueous stock solutions of the ligand were freshly prepared daily just before the titration experiments by dissolving the substance in deionized, ultrapure (MILLI-Q185 PLUS; from Millipore S. A., 67120 Molsheim, France) CO_2-free water and adding 2 equivalents of NaOH.

The disodium salt of ethylenediamine-*N*,*N*,*N*′,*N*′-tetraacetic acid (Na_2EDTA), potassium hydrogenphthalate, HNO_3, NaOH (Titrisol), and the nitrate salts of Na^+, Mg^{2+}, Ca^{2+}, Sr^{2+}, Ba^{2+}, Mn^{2+}, Co^{2+}, Ni^{2+}, Cu^{2+}, Zn^{2+} and Cd^{2+} (all *pro analysi*) were from Merck AG, Darmstadt, FRG. All solutions were prepared with ultrapure, CO_2-free water.

The buffer solutions (pH 4.00, 7.00, 9.00, based on the NBS scale; now NIST) for calibration were from Metrohm AG, Herisau, Switzerland.

Potentiometric pH titrations

The pH titration curves for the determination of the equilibrium constants in H_2O were recorded with a Metrohm E 536 potentiograph connected to a Metrohm E 535 dosimat and a Metrohm 6.0222.100 combined macro glass electrode. The pH calibration of the instrument was done with the buffers mentioned above. The titer of the NaOH used was determined with potassium hydrogenphthalate.

Determination of the acidity constants of $H_2(PMEDAP)^{\pm}$

The exact concentration of the ligand solutions was in each experiment newly determined by the evaluation of the corresponding titration pairs described below. The direct pH meter readings were used in the calculation of the acidity constants; *i.e.* these constants are so-called practical, mixed or Brønsted constants.[34] Their negative logarithms given for aqueous solutions at $I = 0.1$ M ($NaNO_3$) and 25 °C may be converted into the corresponding concentration constants by subtracting 0.02 from the listed pK_a values;[34] this conversion term contains both the junction potential of the glass electrode and the hydrogen ion activity.[34,35]

The acidity constants $K^{H}_{H_2(PMEDAP)}$ and $K^{H}_{H(PMEDAP)}$ of $H_2(PMEDAP)^{\pm}$ were determined by titrating under N_2 (99.999% pure) 50 ml of aqueous 0.00059 M HNO_3 in the presence and absence of 0.00028 M $PMEDAP^{2-}$ with 1 ml of 0.033 M NaOH (25 °C). The ionic strength of 0.1 M was adjusted with $NaNO_3$. As the difference in NaOH consumption between pairs of solutions, *i.e.* with and without ligand,[34] is evaluated, the ionic product of water (K_w) and the mentioned conversion term do not enter into the calculations.

The acidity constants were calculated with an IBM compatible Pentium desk computer connected to an Epson Stylus 1500 printer (data) as well as a Hewlett-Packard Deskjet 1600CM printer (curves) by a curve-fitting program applying a Newton–Gauss non-linear least-squares fitting procedure. The calculations were carried out between about 20 and 100% neutralization with respect to the equilibrium $H_2(PMEDAP)^{\pm}/H(PMEDAP)^-$ and between 0 and about 97% for $H(PMEDAP)^-/PMEDAP^{2-}$. The results are the averages of 27 pairs of independent titrations.

Determination of stability constants

The exact concentrations of the M^{2+} stock solutions were determined by potentiometric pH titration *via* the EDTA complexes.

The conditions for the determination of the stability constants $K^{M}_{M(H;PMEDAP)}$ and $K^{M}_{M(PMEDAP)}$ were the same as given above for the acidity constants, but $NaNO_3$ was now partly or fully

replaced by $M(NO_3)_2$ ($I = 0.1$ M; 25 °C). The M^{2+} : ligand ratios were 119 : 1 or 99 : 1 for the alkaline earth metal ions, 62 : 1 or 31 : 1 for Mn^{2+}, Co^{2+}, Ni^{2+}, 31 : 1, 15 : 1 or 8 : 1 for Zn^{2+} and Cd^{2+}, and 12 : 1 or 6 : 1 for Cu^{2+}. The Zn^{2+} data were treated especially carefully, since a precipitate formed at higher pH values. This problem occurred, albeit less severely, also in the case of Cd^{2+}. The stability constants were calculated with the above mentioned computer facility by a curve-fitting procedure, taking into account the species H^+, $H_2(PMEDAP)^{\pm}$, $H(PMEDAP)^-$, $PMEDAP^{2-}$, M^{2+}, $M(H;PMEDAP)^+$ and M(PMEDAP). The experimental data were used every 0.1 pH unit starting from about 5% complex formation to a neutralization degree of about 90% with respect to the species $H(PMEDAP)^-$, or until the beginning of the hydrolysis of $M(aq)^{2+}$, which was evident from the titrations without ligand. The individual results for the stability constants showed no dependence on pH or on the excess of the metal ion concentration used. The results are in each case the averages of at least seven independent pairs of titration curves. However, several of the constants given for $M(H;PMEDAP)^+$ complexes must be considered as estimates (see Table 2), since the formation degree of these species was rather low in various instances (see Fig. 3).

NMR line broadening and T_1 measurements

The ^1H NMR experiments were performed at 600.13 MHz on a Bruker DRX-600 spectrometer. Samples of PMEDAP, PMEA and AMP were dissolved in aqueous 0.1 M $NaNO_3$ at concentrations around 3 mM and pH 8.3 adjusted by the addition of NaOH. Final sample volumes of 0.5 ml containing 10% D_2O were transferred to 5 mm NMR tubes. A stock solution of 0.15 mM $Cu(NO_3)_2$ was prepared and aliquots of 1 to 2 μl were added directly into the NMR tube. The samples were thoroughly mixed after each addition before the ^1H NMR spectra were recorded. Water suppression was performed using the 3-9-19 WATERGATE pulse sequence.[36] The sample temperature was set at 25 °C. A modest exponential multiplication (line broadening = 1 Hz) was applied to the spectral data (Free Induction Decay) before the Fourier transform to improve the signal-to-noise ratio.

The paramagnetic induced line broadening was measured at half-height of the signals and the result is plotted in Fig. 6. Spin–lattice (T_1) measurements were carried out by the non-selective inversion-recovery technique using 13 τ values in the range 10 ms–10 s. The T_1 results plotted in Fig. 7 are in qualitative agreement with the line-broadening data (Fig. 6).

Results and discussion

1 Dissociation properties of $H_2(PMEDAP)^{\pm}$

Derivatives of purines are well known to undergo self-association *via* π stacking;[37] however, the concentration[21c] of 2.8×10^{-4} M as used in this study for PMEDAP ascertains that only the properties of the monomeric species are quantified. From PMEA and related compounds it is known[16] that the species with a proton at N1 and a twofold protonated phosphonate group can still be protonated further, namely at N7 and N3. However, the deprotonation of these $(N7)H^+$ and $(N3)H^+$ sites occurs with $pK_a < 0$.[16,38] Furthermore, the release of the first proton of the twofold protonated phosphonate group occurs in $H_3(PMEA)^+$ with $pK^H_{H_3(PMEA)} = 1.2$;[16] a similar value may be expected for $H_3(PMEDAP)^+$. Hence, in the pH range of this study, from about 3.5 to 9, only two deprotonation reactions, (2a) and (3a), in which $PMEDAP^{2-}$ is abbreviated as

$$H_2(PA)^{\pm} \rightleftharpoons H(PA)^- + H^+ \quad (2a)$$

$$K^H_{H_2(PA)} = [H(PA)^-]\,[H^+]/[H_2(PA)^{\pm}] \quad (2b)$$

Table 1 Negative logarithms of the acidity constants of $H_2(PMEDAP)^{\pm}$ [equilibria (1) and (2)] together with the corresponding values of some related systems in aqueous solution (25 °C; $I = 0.1$ M, $NaNO_3$)[a,b]

No.	Protonated species	$pK^H_{H_2(PA)}$ $(N1)H^+$	$pK^H_{H(PA)}$ $P(O)_2(OH)^-$	Ref.
1	$H(DAP)^+$	4.98[c]		39[c]
2	$H(PME)^-$		7.02 ± 0.01	17
3	$H_2(PMEDAP)^{\pm}$	4.82 ± 0.01	6.94 ± 0.01	—
4	$H_2(PMEA)^{\pm}$	4.16 ± 0.02	6.90 ± 0.01	17
5	$H_2(AMP)^{\pm}$	3.84 ± 0.02	6.21 ± 0.01	21(*a*)
6	$H(adenine)^+$	4.2		39,41
7	$CH_3OP(O)_2(OH)^-$		6.31 ± 0.01	42

[a] The error limits given are three times the standard error of the mean value or the sum of the probable systematic error, whichever is larger. [b] So-called practical, mixed or Brønsted constants are listed (see also Experimental section). [c] 25 °C; $I = 0.05$ M, $NaClO_4$; this value agrees well with $pK^H_{H(DAP)} = 5.02 \pm 0.10$ given in ref. 40 (20 °C; $I = 0.01$ M).

$$H(PA)^- \rightleftharpoons PA^{2-} + H^+ \quad (3a)$$

$$K^H_{H(PA)} = [PA^{2-}]\,[H^+]/[H(PA)^-] \quad (3b)$$

PA^{2-}, need to be considered. Indeed, all the experimental data obtained from the potentiometric pH titrations in aqueous solution (25 °C; $I = 0.1$ M, $NaNO_3$) could be excellently fitted by taking into account equilibria (2) and (3). The resulting acidity constants of $H_2(PMEDAP)^{\pm}$ are given in Table 1 together with some related data.[39–42]

The release of the first proton in $H_2(PMEDAP)^{\pm}$ occurs from the nucleobase, *i.e.* most likely from the $(N1)H^+$ site as is the case with adenines;[16,41,43] this conclusion agrees with an earlier one[40] and is also borne out by a comparison of the results listed in columns 3 and 4 of Table 1. The addition of a further amino group to the adenine ring leads to the expected increase in basicity (compare entries 6 with 1 and 4 with 3 in Table 1) corresponding also to the observations made with pyridine ($pK^H_{H(Py)} = 5.26$)[44a] and 2-aminopyridine[44b] ($pK^H_{H(2APy)} = 6.96$).[45]

The most basic site in $PMEDAP^{2-}$ is clearly the phosphonate group, which is also slightly more basic than a phosphate group (*cf.* entries 3, 5 and 7 in column 4 of Table 1), since a C–P bond is less polar than an O–P bond. This difference in basicity affects somewhat the formation degree of the free ligands in the physiological pH range around 7.5; *e.g.* deprotonated $PMEDAP^{2-}$ reaches under these conditions a formation degree of only about 80% whereas AMP^{2-} is formed to about 95%. However, this difference has little impact on the formation degree of the M(PA) complexes of these ligands in the physiological pH range.

2 Stability constants of the $M(H;PMEDAP)^+$ and M(PMEDAP) complexes

The potentiometric pH titrations carried out (see Experimental section) allow the determination of the stability constants defined by equilibria (4) and (5). Overall, equilibria (2)–(5) are

$$M^{2+} + H(PA)^- \rightleftharpoons M(H;PA)^+ \quad (4a)$$

$$K^M_{M(H;PA)} = [M(H;PA)^+]/[M^{2+}]\,[H(PA)^-] \quad (4b)$$

$$M^{2+} + PA^{2-} \rightleftharpoons M(PA) \quad (5a)$$

$$K^M_{M(PA)} = [M(PA)]/[M^{2+}]\,[PA^{2-}] \quad (5b)$$

sufficient to obtain excellent fitting of the titration data, provided the evaluation is not carried into the pH range where formation of hydroxo species occurs, which was evident from titrations without ligand. Of course, equilibria (4a) and (5a) are also connected *via* equilibrium (6a) and the corresponding

Table 2 Logarithms of the stability constants of the M(H;PMEDAP)$^+$ [eqn. (4b)] and M(PMEDAP) complexes [eqn. (5b)], together with the negative logarithms of the acidity constants of the protonated complexes [eqns. (6b) and (9)] in aqueous solution at 25 °C and $I = 0.1$ M ($NaNO_3$)[a]

M^{2+}	log $K^{M}_{M(H;PMEDAP)}$	log $K^{M}_{M(PMEDAP)}$	$pK^{H}_{M(H;PMEDAP)}$
Mg^{2+}	0.5 ± 0.3[b]	1.89 ± 0.04	5.6 ± 0.3
Ca^{2+}	0.4 ± 0.3[b]	1.67 ± 0.04	5.7 ± 0.3
Sr^{2+}	0.0 ± 0.5[b]	1.38 ± 0.02	5.6 ± 0.5
Ba^{2+}	0.0 ± 0.5[b]	1.33 ± 0.05	5.6 ± 0.5
Mn^{2+}	0.8 ± 0.3	2.51 ± 0.03	5.2 ± 0.3
Co^{2+}	0.96 ± 0.12	2.43 ± 0.04	5.47 ± 0.13
Ni^{2+}	1.30 ± 0.14	2.60 ± 0.06	5.64 ± 0.15
Cu^{2+}	1.88 ± 0.07	3.94 ± 0.04	4.88 ± 0.08
Zn^{2+}	1.56 ± 0.27[c]	2.78 ± 0.09[c]	5.7 ± 0.3
Cd^{2+}	1.53 ± 0.15[c]	3.00 ± 0.12[c]	5.5 ± 0.2

[a] For the error limits see footnote *a* of Table 1. The error limits (3σ) of the derived data, in the present case for column 4, were calculated according to the error propagation after Gauss. [b] Estimate (see Experimental section). [c] The experiment with Zn^{2+} was significantly hampered by precipitation; *i.e.* the pH range accessible for the evaluation of the constants was restricted. The same problem, though less severe, occurred also with Cd^{2+}.

$$M(H;PA)^+ \rightleftharpoons M(PA) + H^+ \qquad (6a)$$

$$K^{H}_{M(H;PA)} = [M(PA)]\,[H^+]/[M(H;PA)^+] \qquad (6b)$$

acidity constant [eqn. (6b)] may be calculated with eqn. (7).

$$pK^{H}_{M(H;PA)} = pK^{H}_{H(PA)} + \log K^{M}_{M(H;PA)} - \log K^{M}_{M(PA)} \qquad (7)$$

The results listed in Table 2 show the usual trends: the stability of the M(PMEDAP) complexes for the alkaline earth ions decreases with increasing ionic radii indicating that metal ion binding at the phosphonate group is (at least) in part inner-sphere. For the divalent 3d metal ions the long-standing experience[46] is confirmed that the stabilities of phosph(on)ate–metal ion complexes often do not strictly follow[17,20–22,28] the Irving–Williams sequence,[47] an observation in accord with the fact that in ligands of this kind always the phosph(on)ate group is the main binding site[17–22,26] in M(PA) complexes. The stabilities of the monoprotonated M(H;PMEDAP)$^+$ complexes do follow the Irving–Williams sequence and this observation will again be considered below (Section 3; final paragraph).

Fig. 3 (top) shows, as an example, for the Mg^{2+}/PMEDAP system the formation degree of the various species as a dependence on pH. Comparison with the corresponding results for the Mg^{2+}/AMP system in the lower part of Fig. 3 reveals that in the physiological pH range in both systems the Mg(PA) complexes dominate. It is remarkable, however, that despite the higher affinity of $PMEDAP^{2-}$ for protons the formation degree of Mg(PMEDAP) at pH 7.5 is approximately 10% higher than that of Mg(AMP) (66 *versus* 57%). This clearly indicates an increased stability of the Mg(PMEDAP) species which will be discussed in detail in Sections 5 and 6.

3 Co-ordination pattern of the monoprotonated M(H;PMEDAP)$^+$ complexes

It is evident that the evaluation of potentiometric pH titration data only allows one to determine the distribution of species of a net charge type, such as M(H;PMEDAP)$^+$, as well as their stability constant. Hence, further information is required to detect the binding sites of the proton and the metal ion. At first one may ask where the proton is located because binding of a metal ion to a protonated ligand commonly leads to an acidification of the ligand-bound proton. Indeed, the acidity constants of the M(H;PMEDAP)$^+$ complexes given in column 4 of

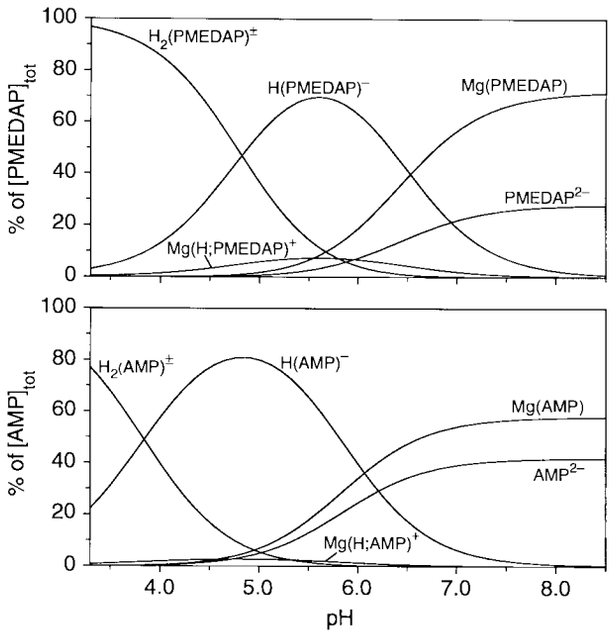

Fig. 3 Effect of pH on the concentration of the species present in the Mg^{2+} systems with PMEDAP (upper part) and AMP (lower part); the results are given as the percentage of the total ligand concentration present. The calculations for PMEDAP were done with the determined acidity (Table 1) and stability constants (Table 2) by using $[PMEDAP]_{tot} = 0.00028$ M and $[Mg^{2+}]_{tot} = 0.03333$ M (concentrations which correspond to the experimental conditions); those for AMP were carried out for the corresponding concentrations using the acidity constants given in Table 1 and the stability constants log $K^{Mg}_{Mg(H;AMP)} = 0.0$ and log $K^{Mg}_{Mg(AMP)} = 1.62$ [see pages 158 and 159 of ref. 22(*b*)].[21c]

Table 2 are by 1.2 to 2 log units smaller than $pK^{H}_{H(PMEDAP)}$ (Table 1), but 0.1 to 0.9 log units larger than $pK^{H}_{H_2(PMEDAP)}$. This indicates that the proton in M(H;PMEDAP)$^+$ is mainly bound to the phosphonate group. Hence, one tentatively may assume that the metal ion is bound preferentially to the nucleobase, since a monoprotonated phosphonate group is only a weak binding site and at least the M(H;PMEDAP)$^+$ complexes of Ni^{2+}, Cu^{2+}, Zn^{2+} and Cd^{2+} are relatively stable (Table 2). Indeed, this suggestion agrees with evidence obtained previously for other related M(H;PA)$^+$ species.[17,19,26,48]

The lack of stability constants of complexes formed with a 9-substituted 2,6-diaminopurine derivative[49] prevents detailed analysis *via* microconstants.[50] However, for several M(H;PMEA)$^+$ complexes evidence has been provided[17–19] that the metal ion is mainly located at the nucleobase and the proton at the phosphate residue. Therefore, we compare the stabilities of those M(H;PMEDAP)$^+$ and M(H;PMEA)$^+$ complexes in Table 3 for which relatively reliable values are available. From the fourth column it is evident that the M(H;PMEDAP)$^+$ complexes are between about 0.3 to 0.5 log units more stable than the corresponding M(H;PMEA)$^+$ species, which is reasonable because the 2,6-diaminopurine moiety is by $\Delta\ pK_a = pK^{H}_{H_2(PMEDAP)} - pK^{H}_{H_2(PMEA)} = (4.82 \pm 0.01) - (4.16 \pm 0.02) = 0.66 \pm 0.02$ more basic than the adenine residue. Furthermore, from log K^{M}_{ML} *versus* pK^{H}_{HL} plots for imidazole- and pyridine-like ligand series it is known[41a,51,52] that the slope (m) of the corresponding straight lines varies between about 0.2 for Mn^{2+} and 0.5 for Cu^{2+} complexes; hence, the expected stability increases for the M(H;PMEDAP)$^+$ complexes are about 0.13 and 0.33 log units for Mn^{2+} and Cu^{2+}, respectively, and for the other metal ions in Table 3 they are in between.

Considering the large error limits given with the differences listed in column 4 of Table 3, the observed and expected stability increases agree surprisingly well. Hence, one may conclude that also in the M(H;PMEDAP)$^+$ complexes the metal ion is mainly bound to the nucleobase moiety and the proton to the phosphonate group. The N1 *versus* N7 dichotomy for metal ion

Table 3 Stability constant comparisons for some monoprotonated $M(H;PMEDAP)^+$ and $M(H;PMEA)^+$ complexes. All constants refer to aqueous solution at 25 °C and $I = 0.1$ M ($NaNO_3$)[a]

M^{2+}	$\log K^{M}_{M(H;PMEDAP)}$[b]	$\log K^{M}_{M(H;PMEA)}$[c]	$\Delta \log K_{(PMEDAP-PMEA)}$[d]
Mn^{2+}	0.8 ± 0.3	0.3 ± 0.5	0.5 ± 0.6
Co^{2+}	0.96 ± 0.12	0.59 ± 0.12	0.37 ± 0.17
Ni^{2+}	1.30 ± 0.14	0.96 ± 0.23	0.34 ± 0.27
Cu^{2+}	1.88 ± 0.07	1.48 ± 0.16	0.40 ± 0.17
Zn^{2+}	1.56 ± 0.27	—[e]	—[f]
Cd^{2+}	1.53 ± 0.15	1.00 ± 0.21	0.53 ± 0.26

[a] Regarding the error limits (3σ) see footnote *a* of Tables 1 and 2. [b] Values from column 2 of Table 2. [c] From ref. 17. [d] Difference between the values in the two columns to the left. [e] Value not available because of the formation of a precipitate in the experiments.[17] [f] If one applies the average of the differences obtained for the complexes of Co^{2+}, Ni^{2+}, Cu^{2+} and Cd^{2+} (0.41) and deducts this value from that available for log $K^{Zn}_{Zn(H;PMEDAP)}$ one obtains an estimate for the stability of $Zn(H;PMEA)^+$, *i.e.* $\log K^{Zn}_{Zn(H;PMEA)} \approx 1.15 \pm 0.3$. This value may be helpful for evaluations to be made in the future.

binding to the adenine residue is well known;[41a,51] for the 2,6-diaminopurine moiety one may expect that N7 is even more favored than in the adenine residue because of the additional steric inhibition which the amino group at C2 exerts on the N1 site. In any case, the fact that the stabilities of the M(H;PMEDAP)$^+$ complexes follow the Irving–Williams sequence[35] (in contrast to phosph(on)ate complexes) also indicates[46a] that metal ion binding occurs to a nitrogen atom.

4 Proof of an enhanced stability of the M(PMEDAP) complexes

For several PME derivatives[17–20,26] as well as for their parent nucleotides,[21,22] the phosph(on)ate group has been identified as the primary binding site in the complexes formed with the deprotonated ligands; this is also true for the M(PMEDAP) complexes as already indicated in Section 2. However, the various additional potential binding sites of $PMEDAP^{2-}$ (see Fig. 2) might also participate in metal ion binding giving rise to chelate formation. Such additional interactions are always reflected in an increased complex stability.[53] Hence, it is necessary to define the stability of a pure $-PO_3^{2-}/M^{2+}$ interaction. This can be done by applying the previously defined[17,20a,22b] straight-line correlations which are based on $\log K^{M}_{M(R\text{-}PO_3)}$ *versus* $pK^{H}_{H(R\text{-}PO_3)}$ plots for simple phosphate monoesters[54] and phosphonates;[17] these ligands are abbreviated as $R\text{–}PO_3^{2-}$, where R represents a non-co-ordinating residue. The parameters for the corresponding straight-line equations, which are defined by eqn. (8), have been tabulated,[17,20a,22b] *i.e.* the slopes *m* and the

$$\log K^{M}_{M(R\text{-}PO_3)} = m \cdot pK^{H}_{H(R\text{-}PO_3)} + b \qquad (8)$$

intercepts *b* with the *y* axis. Hence, with a known pK_a value for the deprotonation of a $-P(O)_2(OH)^-$ group an expected stability constant can be calculated for any phosph(on)ate–metal ion complex.

The plots of $\log K^{M}_{M(R\text{-}PO_3)}$ *versus* $pK^{H}_{H(R\text{-}PO_3)}$ according to eqn. (8) are shown in Fig. 4 for the 1:1 complexes of Ba^{2+}, Mg^{2+}, Ni^{2+} and Cu^{2+}, as examples, with the data points (empty circles) of the eight simple ligand systems used for the determination of the straight baselines. The four solid points, which refer to the corresponding M(PMEDAP) complexes, are significantly above their reference lines, thus proving an increased stability for these complexes. The same is true for the complexes formed with PME^{2-} and $PMEA^{2-}$, but not for those of AMP^{2-}; in the latter case only the complexes of Ni^{2+} and Cu^{2+} are more stable whereas those of Mg^{2+} and Ba^{2+} show the stability expected on the basis of the basicity of the phosphate group of AMP^{2-}. This then indicates that there are differences in the stability, and consequently also in the structure, between the complexes of the parent nucleotide and its synthetic analogues (see also Conclusion).

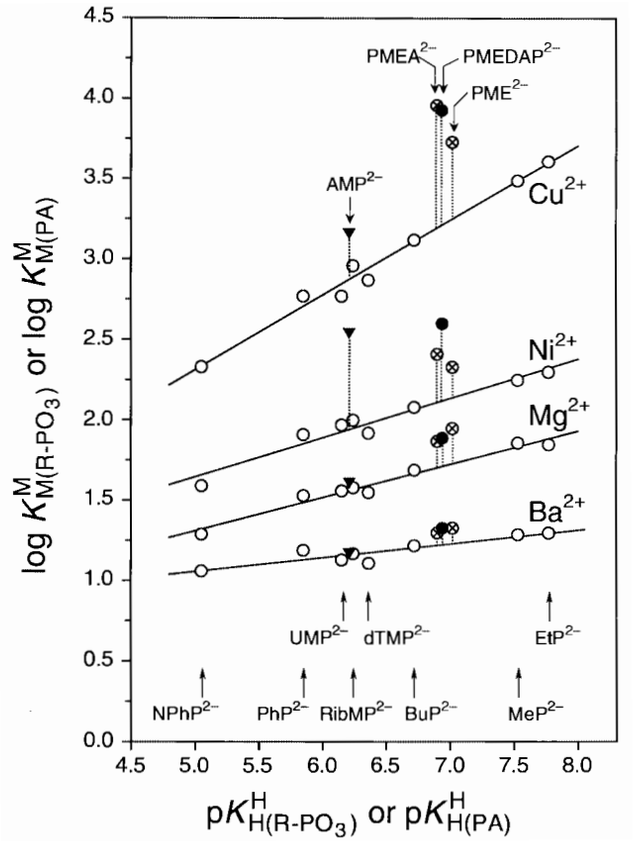

Fig. 4 Evidence for an enhanced stability of the M(PMEDAP) complexes of Ba^{2+}, Mg^{2+}, Ni^{2+} and Cu^{2+} (●) together with some examples of closely related systems (⊗, ▼), based on the relationship between log $K^{M}_{M(R\text{-}PO_3)}$ and $pK^{H}_{H(R\text{-}PO_3)}$ for $M(R\text{–}PO_3)$ complexes of some simple phosphate monoester or phosphonate ligands ($R\text{–}PO_3^{2-}$) (○): 4-nitrophenyl phosphate ($NPhP^{2-}$), phenyl phosphate (PhP^{2-}), uridine 5′-monophosphate (UMP^{2-}), D-ribose 5-monophosphate ($RibMP^{2-}$), thymidine [= 1-(2-deoxy-β-D-ribofuranosyl)thymine] 5′-monophosphate ($dTMP^{2-}$), *n*-butyl phosphate (BuP^{2-}), methanephosphonate (MeP^{2-}), and ethanephosphonate (EtP^{2-}) (from left to right). The least-squares lines [eqn. (8)] are drawn through the corresponding 8 data sets taken from ref. 54 for the phosphate monoesters and from ref. 17 for the phosphonates. The points due to the equilibrium constants for the M^{2+}/PMEDAP systems (●) are based on the values listed in Tables 1 and 2; those for the other M^{2+}/PA systems are from the literature: PME (⊗, ref. 17), PMEA (⊗, ref. 17) and AMP [▼, ref. 22(*b*); see also ref. 21]. The vertical broken lines emphasize the stability differences from the reference lines; they equal log $\Delta_{M/PMEDAP}$ as defined in eqn. (9) for the M(PMEDAP) complexes. All the plotted equilibrium constants refer to aqueous solutions at 25 °C and $I = 0.1$ M ($NaNO_3$).

The stability enhancements seen in Fig. 4 can be quantified by the differences between the experimentally (exptl) measured stability constants and those calculated (calcd) according to eqn. (8); this difference is defined in eqn. (9), where the

$$\log \Delta_{M/PA} = \log K^{M}_{M(PA)_{exptl}} - \log K^{M}_{M(PA)_{calcd}} \qquad (9a)$$

$$= \log K^{M}_{M(PA)} - \log K^{M}_{M(PA)_{op}} \qquad (9b)$$

expressions $\log K^{M}_{M(PA)_{calcd}}$ and $\log K^{M}_{M(PA)_{op}}$ are synonymous because the calculated value equals the stability constant of the 'open' isomer, $M(PA)_{op}$ [see equilibrium (1)], in which only a $-PO_3^{2-}/M^{2+}$ interaction occurs. In columns 2–4 of Table 4 the values for the three terms of eqn. (9) are listed. Since all values for log $\Delta_{M/PMEDAP}$ (column 4) are positive, chelate formation occurs with all the metal ion complexes considered.

5 Source of the increased stability of the M(PMEDAP) complexes

A comparison of the log $\Delta_{M/PME}$ values obtained previously[17] for the complexes of the nucleobase-free PME^{2-} (Table 4,

Table 4 Stability constant comparisons for the M(PMEDAP) complexes between the measured stability constants (exptl; Table 2, column 3) and the calculated stability constants (calcd) based on the basicity of the phosphonate group in $PMEDAP^{2-}$ ($pK^{H}_{H(PMEDAP)} = 6.94$; Table 1) and the baseline equations established previously[17,20a] (see text in Section 4 and Fig. 4), together with the resulting evidence for an increased complex stability, log $\Delta_{M/PMEDAP}$, as defined by eqn. (9). The previously determined stability enhancements for M(PME) complexes (log $\Delta_{M/PME}$)[17] and M(PME-R) complexes (log $\Delta_{M/PME-R}$),[26] where R represents a non-co-ordinating nucleobase residue, are given for comparison. The values for Δ log Δ [eqn. (10)] listed in the final column result from the comparison between the stability enhancements observed for the M(PMEDAP) and M(PME-R) complexes (aqueous solution; 25 °C; $I = 0.1$ M, $NaNO_3$)[a]

	log $K^{M}_{M(PMEDAP)}$					
M^{2+}	exptl	calcd	log $\Delta_{M/PMEDAP}$	log $\Delta_{M/PME}$	log $\Delta_{M/PME-R}$	Δ log Δ
Mg^{2+}	1.89 ± 0.04	1.72 ± 0.03	0.17 ± 0.05	0.22 ± 0.03	0.16 ± 0.04	0.01 ± 0.06
Ca^{2+}	1.67 ± 0.04	1.55 ± 0.05	0.12 ± 0.06	0.14 ± 0.05	0.12 ± 0.05	0.00 ± 0.08
Sr^{2+}	1.38 ± 0.02	1.30 ± 0.04	0.08 ± 0.04	0.07 ± 0.05	0.09 ± 0.05	−0.01 ± 0.06
Ba^{2+}	1.33 ± 0.05	1.23 ± 0.04	0.10 ± 0.06	0.10 ± 0.05	0.11 ± 0.05	−0.01 ± 0.08
Mn^{2+}	2.51 ± 0.03	2.33 ± 0.05	0.18 ± 0.06	0.27 ± 0.05	0.19 ± 0.06	−0.01 ± 0.08
Co^{2+}	2.43 ± 0.04	2.10 ± 0.06	0.33 ± 0.07	0.29 ± 0.06	0.20 ± 0.06	0.13 ± 0.09
Ni^{2+}	2.60 ± 0.06	2.12 ± 0.05	0.48 ± 0.08	0.19 ± 0.05	0.14 ± 0.07	0.34 ± 0.11
Cu^{2+}	3.94 ± 0.04	3.21 ± 0.06	0.73 ± 0.07	0.48 ± 0.07	0.48 ± 0.07	0.25 ± 0.10
Zn^{2+}	2.78 ± 0.09	2.38 ± 0.06	0.40 ± 0.11	0.34 ± 0.06	0.29 ± 0.07	0.11 ± 0.13
Cd^{2+}	3.00 ± 0.12	2.68 ± 0.05	0.32 ± 0.13	0.30 ± 0.05	0.30 ± 0.05	0.02 ± 0.14

[a] Regarding the error limits (3σ) see footnote *a* of Tables 1 and 2.

column 5), with those listed for log $\Delta_{M/PMEDAP}$ reveals that the stability enhancements are identical within the error limits, except for the Ni^{2+} and Cu^{2+} systems. Since, aside from the phosphonate group, only the ether oxygen can bind metal ions in PME^{2-}, evidently 5-membered chelates form and therefore equilibrium (1) operates and this then is also true for the M(PMEDAP) complexes.

However, there is an even more appropriate comparison possible: recently, we studied in detail the M^{2+}/PMEC system[26] and it turned out that in none of the M(PMEC) complexes the cytosine residue (Fig. 1) participates in metal ion binding, but instead in several cases it led to a slight steric hindrance concerning the metal ion–oxygen ether interaction, *i.e.* several of the log $\Delta_{M/PMEC}$ values were somewhat smaller than those obtained for log $\Delta_{M/PME}$. A combination of the values determined for both series enabled us[26] to define log $\Delta_{M/PME-R}$ values for complexes formed with $PME\text{-}R^{2-}$, *i.e.* for a PME^{2-} derivative which carries a non-co-ordinating nucleobase residue R that exhibits, however, in the case of several metal ions (*cf.* columns 5 and 6 in Table 4) a slight steric hindrance. Obviously, these values for log $\Delta_{M/PME-R}$ are the most appropriate ones for a comparison with those of log $\Delta_{M/PMEDAP}$; therefore, we have calculated for the various complex systems the difference Δ log Δ as defined in eqn. (10).

$$\Delta \log \Delta = \log \Delta_{M/PMEDAP} - \log \Delta_{M/PME\text{-}R} \qquad (10)$$

These differences, which are given in the final column to the right in Table 4, are clearly zero within their error limits for the complexes of the alkaline earth ions, Mn^{2+} and Cd^{2+}, thus proving that in the corresponding M(PMEDAP) complexes only equilibrium (1) operates. The additional stability enhancement of about 0.1 to 0.3 log units observed for the M(PMEDAP) complexes of Co^{2+}, Ni^{2+} and Cu^{2+} (and possibly also Zn^{2+}; see Table 6) must be attributed to a further metal ion interaction, namely with the 2,6-diaminopurine residue (Fig. 2) (see Section 7).

6 Evaluation of the M(PMEDAP) stabilities for the isomeric equilibrium (1)

Since the observed stability increase (log $\Delta_{M/PMEDAP}$; Table 4) for the complexes of the alkaline earth ions, and those of Mn^{2+} and Cd^{2+}, is to be attributed solely to an interaction with the ether oxygen, the 5-membered chelate according to equilibrium (1) is the only source of stabilization in the corresponding M(PMEDAP) species.

However, since the extent of these stability enhancements (log $\Delta_{M/PMEDAP}$) depends on the metal ion, the ratio of the two isomers occurring in equilibrium (1) must also vary, and consequently, a quantification of the situation is needed. If we denote the chelated species with the ether–oxygen interaction as $M(PMEDAP)_{cl/O}$ and if we recall that the 'open' species has been termed $M(PMEDAP)_{op}$ (Section 4), the intramolecular and therefore dimensionless equilibrium constant K_I for the concentration-independent equilibrium (1) can be defined as in eqn. (11). The connection between the various stability

$$K_I = [M(PMEDAP)_{cl/O}]/[M(PMEDAP)_{op}] \qquad (11)$$

constants as well as the stability enhancement [eqn. (9)] and K_I is given by (12a); its detailed derivation has been described

$$K_I = \frac{K^{M}_{M(PA)}}{K^{M}_{M(PA)_{op}}} - 1 = 10^{\log \Delta_{M/PA}} - 1 \qquad (12a)$$

previously.[17,20] The formation degree of the closed isomer occurring in equilibrium (1) follows from eqn. (13).

$$\%\ M(PA)_{cl/O} = 100K_I/(1 + K_I) \qquad (13)$$

The results listed in columns 3 and 4 of Table 5 show that the isomers with the 5-membered chelate, having formation degrees between about 15 and (at least) 50%, play a significant role. Of course, a similar chelate formation is not possible in M(AMP) complexes (Fig. 1) (see also Conclusion). The percentages for the M(PMEDAP) complexes of Co^{2+}, Ni^{2+} and Cu^{2+} are given in parentheses in Table 5 to remind us that they include a contribution from a further, *i.e.* a nucleobase–metal ion, interaction.

7 Possible metal ion-binding schemes involving the 2,6-diaminopurine residue

The Δ log Δ values in Table 4 (column 7) reveal that Co(PMEDAP), Ni(PMEDAP) and Cu(PMEDAP) are more stable than the corresponding M(PME-R) complexes, which must mean that a third metal ion-binding site is involved. Since the only difference between $PMEDAP^{2-}$ and $PME\text{-}R^{2-}$ (or PME^{2-}) is the 2,6-diaminopurine residue, this third binding site must be sought here.

At this point it may be helpful to recall some previous results[17–22] concerning the structures of the complexes of the related ligands AMP^{2-} and $PMEA^{2-}$ (Fig. 1), the data points of which have also been included in Fig. 4: the Ni(AMP) and Cu(AMP) complexes show an enhanced stability which results from the formation of a macrochelate involving N7 of the

Table 5 Extent of chelate formation according to equilibrium (1) for the M(PMEDAP) complexes as quantified by the dimensionless equilibrium constant K_I [eqns. (11), (12a)] and the percentages of $M(PMEDAP)_{cl}$ [eqn. (13)] in aqueous solution at 25 °C and $I = 0.1$ M ($NaNO_3$)[a,b]

M^{2+}	$\log \Delta_{M/PMEDAP}$	K_I	% $M(PMEDAP)_{cl/O}$
Mg^{2+}	0.17 ± 0.05	0.48 ± 0.17	32 ± 8
Ca^{2+}	0.12 ± 0.06	0.32 ± 0.19	24 ± 11
Sr^{2+}	0.08 ± 0.04	0.20 ± 0.12	17 ± 9
Ba^{2+}	0.10 ± 0.06	0.26 ± 0.19	21 ± 12
Mn^{2+}	0.18 ± 0.06	0.51 ± 0.20	34 ± 9
Co^{2+}	(0.33 ± 0.07)[b]	(1.14 ± 0.36)	(53 ± 8)
Ni^{2+}	(0.48 ± 0.08)[b]	(2.02 ± 0.54)	(67 ± 6)
Cu^{2+}	(0.73 ± 0.07)[b]	(4.37 ± 0.89)	(81 ± 3)
Zn^{2+}	0.40 ± 0.11[c]	1.51 ± 0.63[c]	60 ± 10[c]
Cd^{2+}	0.32 ± 0.13	1.09 ± 0.63	52 ± 14

[a] Regarding the error limits (3σ) see footnote *a* of Tables 1 and 2. The values in column 2 are from column 4 of Table 4. [b] The parentheses indicate that in these systems also a metal ion–nucleobase interaction is present (see Sections 7–9 and Table 6) and hence the stability increase cannot be solely attributed to equilibrium (1). [c] The stability of Zn(PMEDAP) contains most probably also a contribution from a nucleobase–Zn^{2+} interaction (see Table 6 and also footnote *b* in the same table).

already phosphate-bound metal ion.[21,22] Also the Ni^{2+} and Cu^{2+} complexes of $PMEA^{2-}$ are more stable than the corresponding PME^{2-} complexes (Fig. 4). Indeed, previously we have shown[17,20] that the nucleobase also participates in metal ion binding of $PMEA^{2-}$, but with this ligand N3 is the preferred binding site;[18] the 5-membered chelate involving the ether oxygen can orientate itself into such a position that a simultaneous interaction with N3 becomes favorable; binding to N7 would require the destruction of the 5-membered chelate. Chelate formation of a phosph(on)ate-bound metal ion with N1 is sterically not possible, neither in AMP^{2-} nor in $PMEA^{2-}$ complexes.[17,20]

Considering these observations we are left with the following two possibilities regarding the 2,6-diaminopurine moiety and the formation of further chelated isomer(s) involving the nucleobase: (1) the 5-membered chelate seen in equilibrium (1) remains intact, but forms a further 7-membered chelate involving N3, which is designated as $M(PA)_{cl/O/N3}$, and (2) M^{2+} co-ordinated to the phosphonate group, *i.e.* $M(PA)_{op}$, forms a macrochelate with N7, designated as $M(PA)_{cl/N7}$. These two possibilities are summarized in the equilibrium schemes (14) and (15). Which of the two schemes is more likely to operate

$$M^{2+} + PA^{2-} \overset{K^{M}_{M(PA)_{op}}}{\rightleftharpoons} M(PA)_{op} \overset{K_{I/O}}{\rightleftharpoons} M(PA)_{cl/O} \qquad (14)$$
$$M(PA)_{op} \overset{K_{I/O/N3}}{\rightleftharpoons} M(PA)_{cl/O/N3}$$

$$M^{2+} + PA^{2-} \overset{K^{M}_{M(PA)_{op}}}{\rightleftharpoons} M(PA)_{op} \begin{cases} \overset{K_{I/O}}{\rightleftharpoons} M(PA)_{cl/O} \\ \overset{K_{I/N7}}{\rightleftharpoons} M(PA)_{cl/N7} \end{cases} \qquad (15)$$

in the M(PMEDAP) complexes? The following five points favor scheme (15). (*i*) The basicity of the nitrogens in a purine (adenine) residue decreases in the order N1 > N7 > N3;[38] hence, metal ion binding to N3 is observed only if the primary binding site is ideally situated for such an interaction, like *e.g.* in 2′-AMP^{2-}.[21b] (*ii*) An *ortho*-amino group next to a pyridine nitrogen rather strongly inhibits metal ion binding due to steric hindrance; *e.g.* in the case of Ni^{2+} and Cu^{2+} complexes, by about 1.5 log units.[55] Hence, the C2 amino group significantly disfavors N3 metal ion binding in M(PMEDAP) compared to M(PMEA). (*iii*) The $\log \Delta_{Ni/PMEDAP}$ value (= 0.48; Table 4, column 4) is considerably larger than $\log \Delta_{Ni/PMEA} = 0.30$;[17] this also indicates an involvement of N7 because binding at N3 is inhibited in $PMEDAP^{2-}$ and consequently the size of the corresponding value should be smaller and not larger. (*iv*) Considering the $\Delta \log \Delta$ values [eqn. (10)] in column 7 of Table 4, it appears that the additional stability enhancement is larger with Ni^{2+} than with Cu^{2+}; this observation corresponds to the situation with AMP^{2-}, IMP^{2-} and GMP^{2-}, where macrochelates with N7 are formed.[21c] (*v*) In contrast to the last point, if N3 is the binding site then the stability enhancement for Cu^{2+} should be much larger than the one for Ni^{2+} as is known from[17] $PMEA^{2-}$ and also from[21b] 2′-AMP^{2-}; however, in the present case this is clearly not so (Table 4, column 7).

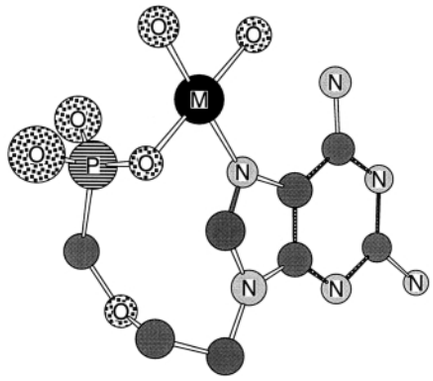

Fig. 5 Simplified structure of the $M(PMEDAP)_{cl/N7}$ macrochelate. The structure was drawn with the program Chem3D Plus (Version 3.5) from Cambridge Scientific Computing Inc.; shown is the minimized and relaxed form.[56]

The above points all favor M^{2+} binding at N7 and hence scheme (15) which contains a macrochelate involving phosphonate and N7 binding. A simplified structure of this $M(PMEDAP)_{cl/N7}$ macrochelate is shown in Fig. 5 which could be drawn in a strain-free way.[56] However, to obtain also direct evidence for the N7 interaction, the experiments described in the next section were carried out.

8 ^{1}H NMR line broadening and T_1 (spin–lattice) measurements with Cu^{2+} confirm N7 binding at the 2,6-diaminopurine residue

To confirm the above conclusions about the various metal ion binding sites at the nucleobase by an independent method, ^{1}H NMR line-broadening experiments were carried out with Cu^{2+}. In the case of $PMEA^{2-}$ such studies[18] have proven very useful to detect the binding site of Cu^{2+} at the adenine residue. In such experiments the ligand is present in vast excess (100–10000) over the paramagnetic metal ion. Provided ligand exchange reactions are fast on the NMR timescale, the ligand molecule switches between a paramagnetic environment (*e.g.* bound to Cu^{2+}, $S = 1/2$) and a "free" state. The interaction of the spin of the unpaired electron of Cu^{2+} with the nuclear spin of neighboring protons gives rise to paramagnetic relaxation, which is reflected in shorter relaxation times [both spin–lattice (T_1) and spin–spin (T_2)], and hence in the broadening of the NMR signals of such protons, the linewidth equaling $\Delta = 1/\pi T_2$. The extent of line broadening is proportional to r^{-6}, where r is the distance between the proton and the paramagnetic metal ion, and thus it is possible to detect the preferred binding sites at a ligand by titrating its solution with increasing amounts of the paramagnetic metal ion.

Unfortunately, application of this method to $PMEDAP^{2-}$ is less straightforward than to $PMEA^{2-}$, since binding to N3 and N7 cannot be compared directly *via* the adjacent H8 and H2 protons because 2,6-diaminopurine lacks H2. However, it is possible to compare in a semiquantitative way the effects of Cu^{2+} on the H8 and H2 signals (where available) of AMP^{2-},

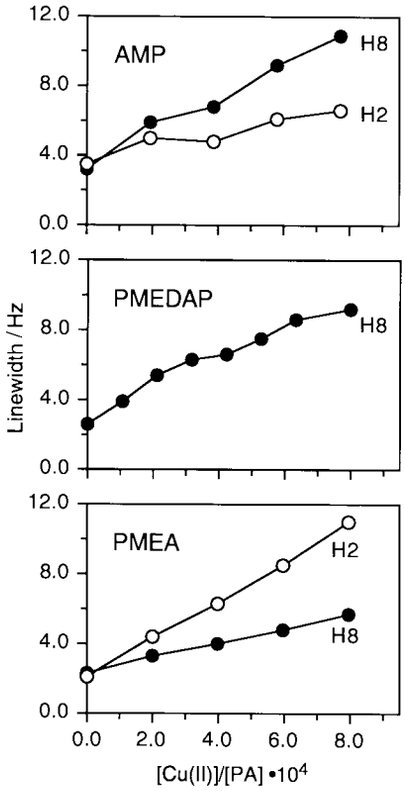

Fig. 6 Effect of increasing amounts of Cu^{2+} on the ^1H NMR linewidths of the aromatic protons of AMP^{2-}, $PMEDAP^{2-}$ and $PMEA^{2-}$. The ^1H NMR line broadening experiments were carried out at 25 °C in H_2O containing 10% D_2O at pH approximately 8.3 with [PA] ≈ 2.8 mM (I = 0.1 M, $NaNO_3$).

$PMEDAP^{2-}$ and $PMEA^{2-}$, as shown in Fig. 6. The following points may be emphasized by keeping in mind that AMP^{2-} forms macrochelates involving N7, $M(AMP)_{cl/N7}$,[21,22] whereas with $PMEA^{2-}$ the species involving N3, $M(PMEA)_{cl/O/N3}$ dominate [scheme (14)];[18] of course, the observed line broadening in such a system may be induced by *both* monodentate metal ion binding *and* chelate formation. (*i*) The line broadening which the signals of H8 experience in $PMEDAP^{2-}$ corresponds to that in AMP^{2-}, indicating that in both instances N7 is the binding site giving rise to $M(PA)_{cl/N7}$ isomers. (*ii*) The extent of the line broadening for H2 of $PMEA^{2-}$ corresponds to that for H8 of $PMEDAP^{2-}$, suggesting that the preferred sites of interaction are N3 for $PMEA^{2-}$ and N7 for $PMEDAP^{2-}$. (*iii*) The smaller line broadening observed for H2 (compared to H8) of AMP^{2-} and also for H8 (compared to H2) of $PMEA^{2-}$ again corresponds in extent to each other; it probably results from the monodentate Cu^{2+} binding at N3 and N7, respectively. (*iv*) The linewidth of the two protons of the C2 amino group in $PMEDAP^{2-}$ showed no dependence on the Cu^{2+} concentration (data not shown).

In Fig. 7 the $1/T_1$ values, measured in the same experiments as the data shown in Fig. 6, are plotted *versus* increasing amounts of Cu^{2+}. It is evident that the signals of H8 of AMP^{2-} are strongly affected in contrast to those of H2, which is in accord with the formation of $Cu(AMP)_{cl/N7}$. In the same figure the measured values for the Cu^{2+}/$PMEDAP^{2-}$ system are inserted; in this case H8 is still significantly affected but not quite as pronounced as H8 of AMP^{2-}. The reason for this is probably that in the Cu^{2+}/PMEDAP system also the isomer with the 5-membered chelate involving the ether oxygen, $Cu(PMEDAP)_{cl/O}$, forms on the account of the N7 interaction [see scheme (15)]. In the Cu^{2+}/AMP^{2-} system no such competition reaction is possible. However, overall the spin–spin relaxation time (T_2; paramagnetic line broadening; Fig. 6) and the spin–lattice relaxation time (T_1; Fig. 7) lead to the same

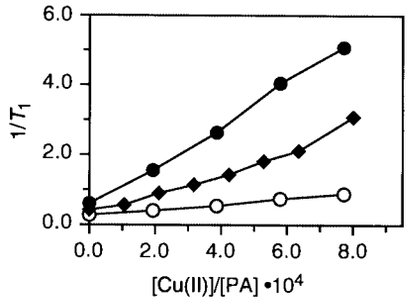

Fig. 7 Effect of increasing amounts of Cu^{2+} on the inverse of the ^1H NMR spin–lattice relaxation time ($1/T_1$) of the protons H8 (◆) of PMEDAP, and H2 (○) and H(8) (●) of AMP. The experiments were carried out at 25 °C in H_2O containing 10% D_2O at pH approximately 8.3 with [PA] ≈ 2.8 mM (I = 0.1 M, $NaNO_3$).

result, namely that the favored metal ion-binding site in the 2,6-diaminopurine residue is N7.

The preceding points together with the reasonings outlined in Section 7 lead us to conclude that N7 is the preferred binding site in the $PMEDAP^{2-}$ systems, thus giving rise to the formation of $M(PMEDAP)_{cl/N7}$ macrochelates. Hence, equilibrium scheme (15) operates and a quantitative evaluation for the formation degrees of the corresponding three isomeric complexes is needed.

9 Quantification of the formation degree of the three isomers occurring in equilibrium scheme (15)

With the values calculated for Δ log Δ [eqn. (10); Table 4, column 7] an extra stability enhancement was determined for the M(PMEDAP) complexes of Co^{2+}, Ni^{2+}, Cu^{2+} and possibly also Zn^{2+}, which is to be attributed to macrochelate formation involving N7 (Sections 7 and 8). Hence, we have to deal with the three isomers, $M(PMEDAP)_{op}$, $M(PMEDAP)_{cl/O}$ and $M(PMEDAP)_{cl/N7}$ which are in equilibrium with each other as described by scheme (15). A closely related three-isomer problem has been treated by us before[17,20] and therefore below only the pertinent definitions are given.

The three equilibrium constants of scheme (15) are defined by eqns. (16)–(18), where (17) corresponds to the previous (11).

$$K^{M}_{M(PA)_{op}} = [M(PA)_{op}]/[M^{2+}]\,[PA^{2-}] \quad (16)$$

$$K_{I/O} = [M(PA)_{cl/O}]/[M(PA)_{op}] \quad (17)$$

$$K_{I/N7} = [M(PA)_{cl/N7}]/[M(PA)_{op}] \quad (18)$$

With these definitions the measured overall stability constant can be redefined as in eqns. (19a)–(19d). The connection

$$K^{M}_{M(PA)} = \frac{[M(PA)]}{[M^{2+}][PA^{2-}]} \quad (19a)$$

$$= \frac{[M(PA)_{op}] + [M(PA)_{cl/O}] + [M(PA)_{cl/N7}]}{[M^{2+}]\,[PA^{2-}]} \quad (19b)$$

$$= K^{M}_{M(PA)_{op}} + K_{I/O}K^{M}_{M(PA)_{op}} + K_{I/N7}K^{M}_{M(PA)_{op}} \quad (19c)$$

$$= K^{M}_{M(PA)_{op}}\,(1 + K_{I/O} + K_{I/N7}) \quad (19d)$$

between K_I which is now more correctly defined as $K_{I/tot}$ and the accessible stability enhancements log $\Delta_{M/PA}$ [eqn. (9); Table 4] is still given by eqn. (12a), which is rewritten below as (12b).

$$K_I = K_{I/tot} = \frac{K^{M}_{M(PA)}}{K^{M}_{M(PA)_{op}}} - 1 = 10^{\log \Delta_{M/PA}} - 1 \quad (12b)$$

Table 6 Intramolecular equilibrium constants for the formation of the various M(PMEDAP) complexes as defined in the equilibrium scheme (15), together with the percentages in which the isomers occur in aqueous solution at 25 °C and $I = 0.1$ M ($NaNO_3$). The values for the M(AMP) complexes[22b] are given for comparison[a]

System	$\log \Delta_{M/PA}$ eqn. (9)	$K_{I/tot}$ eqn. (12b)	% $M(PA)_{cl/tot}$ eqn. (20a)	% $M(PA)_{op}$ eqn. (15), (20a)	$\log \Delta_{M/PME-R}$ eqn. (9)	$K_{I/O}$ eqn. (12a), (17)	% $M(PA)_{cl/O}$ eqn. (1), (13), (15)	$K_{I/N7}$ eqn. (18), (20b)	% $M(PA)_{cl/N7}$ eqn. (15)
Co(PMEDAP)	0.33 ± 0.07	1.14 ± 0.36	53 ± 8	47 ± 8	0.20 ± 0.06	0.58 ± 0.22	27 ± 11	0.55 ± 0.42	26 ± 14
Ni(PMEDAP)	0.48 ± 0.08	2.02 ± 0.54	67 ± 6	33 ± 6	0.14 ± 0.07	0.38 ± 0.22	13 ± 8	1.64 ± 0.59	54 ± 10
Cu(PMEDAP)	0.73 ± 0.07	4.37 ± 0.89	81.4 ± 3	18.6 ± 3	0.48 ± 0.07	2.02 ± 0.49	38 ± 11	2.35 ± 1.02	43 ± 11
Zn(PMEDAP)[b]	0.40 ± 0.11	1.51 ± 0.63	60 ± 10	40 ± 10	0.29 ± 0.07	0.95 ± 0.31	38 ± 16	0.56 ± 0.70	22 ± 19
Co(AMP)	0.36 ± 0.07	1.29 ± 0.38						1.29 ± 0.38	56 ± 7
Ni(AMP)	0.61 ± 0.06	3.07 ± 0.60						3.07 ± 0.60	75 ± 4
Cu(AMP)	0.30 ± 0.06	1.00 ± 0.29						1.00 ± 0.29	50 ± 7
Zn(AMP)	0.25 ± 0.09	0.78 ± 0.38						0.78 ± 0.38	44 ± 12

[a] Regarding the error limits (3σ) see footnote *a* of Tables 1 and 2. The values for the M(AMP) systems are from ref. 22(*b*) [see also ref. 21(*c*)]. As far as $PMEDAP^{2-}$ is concerned, the values in the second column are from column 4 of Table 4. The values given in the fifth column for percentage $M(PA)_{op}$ follow from 100 − % $M(PA)_{cl/tot}$. The constants $K_{I/O}$ result from the M^{2+}/PME-R system and are taken from ref. 26 (see also text in Section 5 and Table 4, column 6); with the now known values for $K_{I/tot}$ and $K_{I/O}$ and eqn. (20b) those for $K_{I/N7}$ may be calculated (column 9). The results for column 8 [% $M(PA)_{cl/O}$] were calculated with eqn. (17) using the known values for $K_{I/O}$ and % $M(PA)_{op}$. The values for the final column to the right [% $M(PA)_{cl/N7}$] follow from the difference in percentages, *i.e.* % $M(PA)_{cl/tot}$ − % $M(PA)_{cl/O}$; for further details see Tables 4 or 11 in refs. 20(*a*) or 17, respectively. [b] The detection of the $Zn(PMEDAP)_{cl/N7}$ isomer is at the limit of the method; however, the formation of this species is most probably real; application of a lower error limit, *i.e.* of 2σ give % $Zn(PMEDAP)_{op} = 40 \pm 7$, % $Zn(PMEDAP)_{cl/O} = 38 \pm 11$, and % $Zn(PMEDAP)_{cl/N7} = 22 \pm 13$.

Hence, $K_{I/tot}$ is known and its relation to the other two intramolecular equilibrium constants is as shown in eqns. (20a) and (20b). Based on the reasonable assumption that the stability of

$$K_I = K_{I/tot} = \frac{[M(PA)_{cl/tot}]}{[M(PA)_{op}]} = \frac{[M(PA)_{cl/O}] + [M(PA)_{cl/N7}]}{[M(PA)_{op}]} \quad (20a)$$

$$= K_{I/O} + K_{I/N7} \quad (20b)$$

the $M(PMEDAP)_{cl/O}$ isomer is well represented by that of the $M(PME\text{-}R)_{cl/O}$ species, $K_{I/O}$ can be calculated with eqn. (12a) (see Section 6) from the known[26] values for log $\Delta_{M/PME\text{-}R}$ (Table 4, column 6) and then $K_{I/N7}$ follows from eqn. (20b). The results are summarized in Table 6, together with the values for the relevant M^{2+}/AMP^{2-} systems.[22b]

As one would expect, the sums of % $M(PMEDAP)_{cl/O}$ and % $M(PMEDAP)_{cl/N7}$ from columns 8 and 10 of Table 6 correspond to the values given in parentheses in Table 5, column 4. It also needs to be pointed out that the formation of some $Zn(PMEDAP)_{cl/N7}$ is most probably real (see row 4 in Table 6); this example demonstrates nicely the importance of a careful error analysis for such an evaluation.

Clearly, the results of Table 6 allow many conclusions, a few are given. The most important one probably is that in all the $PMEDAP^{2-}$ systems considered all three isomers of the M(PMEDAP) complexes [see scheme (15)] are formed in appreciable amounts. In addition, the results emphasize again that Ni^{2+} is more suitable for an N7 interaction than is Cu^{2+}; this contrasts with the N3 binding occurring in M(PMEA) and M(2′-AMP) where Cu^{2+} is favored.[18,21b] Since the structures of $M(PA)_{op}$ and $M(PA)_{cl/N7}$ are quite alike for $PMEDAP^{2-}$ (Fig. 2) and AMP^{2-} (Fig. 1), it is evident that $PMEDAP^{2-}$ resembles in its metal ion-binding properties its parent nucleotide AMP^{2-} more closely than $PMEA^{2-}$ (Fig. 1), where the $M(PMEA)_{cl/O/N3}$ isomers are important.[18] Both nucleotide analogues differ, however, from the M(AMP) complexes as far as the formation of the 5-membered chelates, $M(PA)_{cl/O}$, is concerned.

Conclusion

The analysis of the potentiometric pH titration data reveals clearly that $PMEDAP^{2-}$, like other PME^{2-} derivatives,[17,19,26] is able to act at least as a mono- and bi-dentate ligand as is indicated in equilibrium (1) for all the metal ions studied. The absolute stabilities of the $PMEDAP^{2-}$ complexes are in addition, *i.e.* next to the 5-membered chelate, somewhat further increased, compared to those of the corresponding AMP^{2-} complexes, due to the higher basicity of the phosphonate group compared to a phosphate group. Hence, all M(PMEDAP) complexes reach in the physiological pH range a somewhat higher formation degree than the M(AMP) complexes (see, *e.g.* Fig. 3).

It is safe to assume that the indicated enhanced stability is also retained in the complexes formed by the triphosphate analogue, *i.e.* $PMEDAPpp^{4-}$, if two metal ions are bound to the triphosph(on)ate chain. From crystal structure studies[25] of DNA polymerases in the presence of their substrates, it is known that one Mg^{2+} is bound to the α-phosphate group of the nucleoside 5′-triphosphate substrate and the other one to the β- and γ-phosphate groups. The metal ions, which are also bound to the protein,[25] are thus responsible for the correct orientation of the substrate and they assist in the hydrolysis of the P–O bond between the α- and β-phosphate groups.[29,57]

The indicated ideas concerning the importance of an enhanced metal ion binding to the α-phosph(on)ate group (see also the introductory section)[29] are further supported by the indication[9] that PME derivatives in their diphosphorylated state apparently have, compared to their parent nucleoside 5′-triphosphates, a lower activity with enzymes which cleave between the β- and γ-phosphate groups, such as nucleoside diphosphate kinase or ATPase,[9] as these require the M(α,β)–M(γ) metal ion co-ordination pattern.[57a,b] Further support comes from the knowledge that the ether oxygen responsible for chelate formation [see equilibrium (1)] is compulsory for an antiviral activity; omitting, replacement by sulfur or shifting the position of this oxygen leads to a reduction or even loss of the biological activity.[3,4,58]

Acknowledgements

The competent technical assistance of Mrs. Rita Baumbusch in the preparation of this manuscript is gratefully acknowledged. This study was supported by the Swiss National Science Foundation (H. S.), the Grant Agency of the Czech Republic (grant no. 203/96/K001) (A. H.) and the Norwegian Research Council (E. S.) as well as within the COST D8 programme by the Swiss Federal Office for Education and Science (H. S.), the Ministry of Education of the Czech Republic (A. H.) and the Government of Norway (E. S.).

Notes and references

1 *Abbreviations and definitions*: see Figs. 1 and 2; 2′-AMP^{2-}, adenosine 5′-monophosphate; ANP^{2-}, acyclic nucleoside phosphonate; DAP, 2,6-diaminopurine; *I*, ionic strength; M^{2+}, divalent metal ion; NMP^{2-}, nucleoside 5′-monophosphate; NTP^{4-}, nucleoside 5′-triphosphate; PA, $PMEDAP^{2-}$ or any other twofold negatively charged nucleotide or nucleotide analogue; PME-R^{2-}, PME^{2-} derivative with a (nucleobase) residue R that has no affinity for metal ions; R-PO_3^{2-}, simple phosphate monoester or phosphonate ligand with R representing a non-co-ordinating residue (see also legend of Fig. 4). Species written without a charge either do not carry one or represent the species in general (*i.e.* independent of their protonation degree); which of the two possibilities applies is always clear from the context. In formulae like $M(H;PMEDAP)^+$ H^+ and $PMEDAP^{2-}$ are separated by a semicolon to facilitate reading, yet they appear within the same parenthesis to indicate that the proton is at the ligand without defining its location (see also Section 3).
2 L. Naesens, R. Snoeck, G. Andrei, J. Balzarini, J. Neyts and E. De Clercq, *Antiviral Chem. Chemother.*, 1997, **8**, 1.
3 A. Holý, E. De Clercq and I. Votruba, *ACS Symp. Ser.*, 1989, **401**, 51.
4 (*a*) A. Holý, I. Votruba, A. Merta, J. Černý, J. Veselý, J. Vlach, K. Šedivá, I. Rosenberg, M. Otmar, H. Hřebabecký, M. Trávniček, V. Vonka, R. Snoeck and E. De Clercq, *Antiviral Res.*, 1990, **13**, 295; (*b*) E. De Clercq, T. Sakuma, M. Baba, R. Pauwels, J. Balzarini, I. Rosenberg and A. Holý, *Antiviral Res.*, 1987, **8**, 261.
5 E. De Clercq, *Biochem. Pharmacol.*, 1991, **42**, 963.
6 E. De Clercq, *Collect. Czech. Chem. Commun.*, 1998, **63**, 480.
7 E. De Clercq, *Collect. Czech. Chem. Commun.*, 1998, **63**, 449.
8 P. Barditch-Crovo, J. Toole, C. W. Hendrix, K. C. Cundy, D. Ebeling, H. S. Jaffe and P. S. Lietman, *J. Infect. Dis.*, 1997, **176**, 406.
9 J. Balzarini, Z. Hao, P. Herdewijn, D. G. Johns and E. De Clercq, *Proc. Natl. Acad. Sci. USA*, 1991, **88**, 1499.
10 A. Merta, I. Votruba, J. Jindřich, A. Holý, T. Cihlář, I. Rosenberg, M. Otmar and T. Y. Herve, *Biochem. Pharmacol.*, 1992, **44**, 2067.
11 B. L. Robbins, J. Greenhaw, M. C. Connelly and A. Fridland, *Antimicrob. Agents Chemother.*, 1995, **39**, 2304.
12 T. Cihlář and M. S. Chen, *Mol. Pharmacol.*, 1996, **50**, 1502.
13 S. A. Foster, J. Černý and Y.-c. Cheng, *J. Biol. Chem.*, 1991, **266**, 238.
14 (*a*) P. Kramata, I. Votruba, B. Otová and A. Holý, *Mol. Pharmacol.*, 1996, **49**, 1005; (*b*) J. Neyts and E. De Clercq, *Biochem. Pharmacol.*, 1994, **47**, 39.
15 I. Votruba, R. Bernaerts, T. Sakuma, E. De Clercq, A. Merta, I. Rosenberg and A. Holý, *Mol. Pharmacol.*, 1987, **23**, 524.
16 C. A. Blindauer, A. Holý, H. Dvořáková and H. Sigel, *J. Chem. Soc.*, *Perkin Trans. 2*, 1997, 2353.
17 H. Sigel, D. Chen, N. A. Corfù, F. Gregáň, A. Holý and M. Strašák, *Helv. Chim. Acta*, 1992, **75**, 2634.
18 C. A. Blindauer, A. H. Emwas, A. Holý, H. Dvořáková, E. Sletten and H. Sigel, *Chem. Eur. J.*, 1997, **3**, 1526.
19 C. A. Blindauer, A. Holý, H. Dvořáková and H. Sigel, *J. Biol. Inorg. Chem.*, 1998, **3**, 423.
20 H. Sigel, (*a*) *Coord. Chem. Rev.*, 1995, **144**, 287; (*b*) *J. Indian Chem. Soc.*, 1997, **74**, 261 (P. Ray Award Lecture).
21 (*a*) H. Sigel, S. S. Massoud and R. Tribolet, *J. Am. Chem. Soc.*, 1988, **110**, 6857; (*b*) S. S. Massoud and H. Sigel, *Eur. J. Biochem.*, 1989,

179, 451; (*c*) H. Sigel, S. S. Massoud and N. A. Corfù, *J. Am. Chem. Soc.*, 1994, **116**, 2958.
22 (*a*) H. Sigel, *Chem. Soc. Rev.*, 1993, **22**, 255; (*b*) H. Sigel and B. Song, *Met. Ions Biol. Syst.*, 1996, **32**, 135 [see ref. 24(*a*)].
23 (*a*) A. S. Mildvan, *Magnesium,* 1987, **6**, 28; (*b*) *Compendium on Magnesium and Its Role in Biology, Nutrition, and Physiology*, vol. 26 of *Metal Ions in Biological Systems*, eds. H. Sigel and A. Sigel, Dekker, New York, 1990, pp. 1–744.
24 (*a*) *Interactions of Metal Ions with Nucleotides, Nucleic Acids and Their Constituents*, vol. 32 of *Metal Ions in Biological Systems*, eds. H. Sigel and A. Sigel, Dekker, New York, 1996, pp. 1–814; (*b*) *Interrelations among Metal Ions, Enzymes, and Gene Expression*, vol. 25 of *Metal Ions in Biological Systems*, eds. H. Sigel and A. Sigel, Dekker, New York, 1989, pp. 1–557.
25 H. Pelletier, M. R. Sawaya, W. Wolfle, S. H. Wilson, and J. Kraut, *Biochemistry*, 1996, **35**, 12742; 12762.
26 C. A. Blindauer, A. Holý and H. Sigel, *Collect. Czech. Chem. Commun.*, 1999, **64**, 613.
27 B. Song, S. A. A. Sajadi, F. Gregáň, N. Prónayová and H. Sigel, *Inorg. Chim. Acta*, 1998, **273**, 101.
28 B. Song, J. Zhao, F. Gregáň, N. Prónayová, S. A. A. Sajadi and H. Sigel, *Metal-Based Drugs*, 1999, **6**, in the press.
29 H. Sigel, B. Song, C. A. Blindauer, L. E. Kapinos, F. Gregáň and N. Prónayová, *Chem. Commun.*, 1999, 743; H. Sigel, *Pure Appl. Chem.*, 2000, **72**, in the press.
30 L. Naesens, J. Balzarini, I. Rosenberg, A. Holý and E. De Clercq, *Eur. J. Clin. Microbiol. Infect. Dis.*, 1989, **8**, 1043; E. De Clercq, *Drugs Exptl. Clin. Res.*, 1990, **16**, 319; T. Yokota, S. Mochizuki, K. Konno, S. Mori, S. Shigeta and E. De Clercq, *Antimicrob. Agents Chemother.*, 1991, **35**, 394; J. Neyts, F. Stals, C. Bruggeman and E. De Clercq, *Eur. J. Clin. Microbiol. Infect. Dis.*, 1993, **12**, 437.
31 J. Balzarini, S. Aquaro, C.-F. Perno, M. Witvrouw, A. Holý and E. De Clercq, *Biochem. Biophys. Res. Commun.*, 1996, **219**, 337.
32 J. Veselý, A. Merta, I. Votruba, I. Rosenberg and A. Holý, *Neoplasma*, 1990, **37**, 105; F. Franek, A. Holý, I. Votruba and T. Eckschlager, *Int. J. Oncol.*, 1999, **14**, 745.
33 A. Holý, J. Günter, H. Dvořáková, M. Masojídková, G. Andrei, R. Snoeck, J. Balzarini and E. De Clercq, *J. Med. Chem.*, 1999, **42**, 2064; A. Holý, I. Rosenberg and H. Dvořáková, *Collect. Czech. Chem. Commun.*, 1989, **54**, 2190.
34 H. Sigel, A. D. Zuberbühler and O. Yamauchi, *Anal. Chim. Acta*, 1991, **255**, 63.
35 H. M. Irving, M. G. Miles and L. D. Pettit, *Anal. Chim. Acta*, 1967, **38**, 475.
36 V. Sklenář, M. Piotto, R. Leppik and V. Saudek, *J. Magn. Reson. Ser. A*, 1993, **102**, 241.
37 O. Yamauchi, A. Odani, H. Masuda and H. Sigel, *Met. Ions Biol. Syst.*, 1996, **32**, 207 [see ref. 24(*a*)].
38 (*a*) R. L. Benoit and M. Fréchette, *Can. J. Chem.*, 1984, **62**, 995; (*b*) C. Meiser, B. Song, E. Freisinger, M. Peilert, H. Sigel and B. Lippert, *Chem. Eur. J.*, 1997, **3**, 388.
39 H. Reinert and R. Weiss, *Hoppe-Seyler's Z. Physiol. Chem.*, 1969, **350**, 1310.
40 B. M. Lynch, R. K. Robins and C. C. Cheng, *J. Chem. Soc.*, 1958, 2973.
41 (*a*) R. B. Martin, *Met. Ions Biol. Syst.*, 1996, **32**, 61 [see ref. 24(*a*)]; (*b*) R. B. Martin and Y. H. Mariam, *Met. Ions Biol. Syst.*, 1979, **8**, 57.
42 A. Saha, N. Saha, L.-n. Ji, J. Zhao, F. Gregáň, S. A. A. Sajadi, B. Song and H. Sigel, *J. Biol. Inorg. Chem.*, 1996, **1**, 231.
43 R. Tribolet and H. Sigel, *Eur. J. Biochem.*, 1987, **163**, 353.
44 (*a*) D. Banerjea, T. A. Kaden and H. Sigel, *Inorg. Chem.*, 1981, **20**, 2586; (*b*) M. S. Sun and D. G. Brewer, *Can. J. Chem.*, 1967, **45**, 2729.
45 These observations further support the conclusion that the first nucleobase protonation actually occurs at N1: if one assumes in a first approximation that the additional amino group at C2 affects the basicity of the neighboring N1 and N3 similarly, the basicity increase for the N1 site amounts to $\Delta\ pK_a \approx 0.7$–0.8 (see Table 1), which is reasonable, whereas for the N3 site one would obtain $\Delta\ pK_a > 5$, which cannot be the case; the latter argument applies also for the N7 site.
46 (*a*) H. Sigel and D. B. McCormick, *Acc. Chem. Res.*, 1970, **3**, 201; (*b*) H. Sigel, K. Becker and D. B. McCormick, *Biochem. Biophys. Acta*, 1967, **148**, 655.
47 H. Irving and R. J. P. Williams, *Nature* (*London*), 1948, **162**, 746; *J. Chem. Soc.*, 1953, 3192.
48 M. S. Lüth, L. E. Kapinos, B. Song, B. Lippert and H. Sigel, *J. Chem. Soc., Dalton Trans.*, 1999, 357.
49 (*a*) IUPAC Stability Constants Database, Version 3.02 (compiled by L. D. Pettit and H. K. J. Powell), Academic Software, Timble, Otley, UK, 1998; (*b*) NIST Critically Selected Stability Constants of Metal Complexes, Reference Database 46, Version 5.0 (data collected and selected by R. M. Smith and A. E. Martell), U.S. Department of Commerce, National Institute of Standards and Technology, Gaithersburg, USA, 1998; (*c*) Joint Expert Speciation System (JESS), Version 5.1 (joint venture by K. Murray and P. M. May), Division of Water Technology, CSIR, Pretoria, South Africa, and School of Mathematical and Physical Sciences, Murdoch University, Murdoch, Western Australia, 1996.
50 (*a*) R. B. Martin, *Met. Ions Biol. Syst.*, 1979, **9**, 1; (*b*) B. Song, D. Chen, M. Bastian, R. B. Martin and H. Sigel, *Helv. Chim. Acta*, 1994, **77**, 1738; (*c*) R. K. O. Sigel, B. Song and H. Sigel, *J. Am. Chem. Soc.*, 1997, **119**, 744.
51 H. Sigel, N. A. Corfù, L.-n. Ji and R. B. Martin, *Comments Inorg. Chem.*, 1992, 13, 35.
52 L. E. Kapinos, B. Song and H. Sigel, *Inorg. Chim. Acta* (M. E. Vol'pin Memorial Issue), 1998, **280**, 50; *Chem. Eur. J.*, 1999, **5**, 1794.
53 R. B. Martin and H. Sigel, *Comments Inorg. Chem.*, 1988, **6**, 285.
54 S. S. Massoud and H. Sigel, *Inorg. Chem.*, 1988, **27**, 1447.
55 L.-n. Ji, N. A. Corfù and H. Sigel, *J. Chem. Soc., Dalton Trans.*, 1991, 1367.
56 It is interesting that if one attempts to draw the $M(PMEDAP)_{cl/O/N3}$ species of scheme (14) in the same way with the same Chem3D program, one observes that in the minimized and relaxed form the bond angles around M^{2+} are no longer 90° and those around C2 are strongly distorted, *i.e.* they deviate significantly from 120°, reflecting the steric strain imposed by the N3–M^{2+} bond due to the neighboring $(C2)NH_2$ group.
57 (*a*) H. Sigel, F. Hofstetter, R. B. Martin, R. M. Milburn, V. Scheller-Krattiger and K. H. Scheller, *J. Am. Chem. Soc.*, 1984, **106**, 7935; (*b*) H. Sigel, *Coord. Chem. Rev.*, 1990, **100**, 453, see pp. 529–532; (*c*) H. Pelletier, *Science*, 1994, **266**, 2025; (*d*) T. A. Steitz, *Nature* (*London*), 1998, **391**, 231.
58 D. Villemin and F. Thibault-Starzyk, *Synth. Commun.*, 1993, **23**, 1053.

Paper 9/04838C